Nanotechnology **20** (2009) 125607 (9pp) doi:10.1088/0957-4484/20/12/125607

Growth of segmented gold nanorods with nanogaps by the electrochemical wet etching technique for single-electron transistor applications

Nguyen Van Hoang, Sanjeev Kumar and Gil-Ho Kim[1]

School of Information and Communication Engineering, Sungkyunkwan University, Suwon 440-746, Korea
and
Sungkyunkwan Advanced Institute of Nanotechnology, Sungkyunkwan University, Suwon 440-746, Korea

E-mail: ghkim@skku.edu

Received 22 December 2008, in final form 29 January 2009
Published 4 March 2009
Online at stacks.iop.org/Nano/20/125607

Abstract

The growth of multisegment nanorods comprising gold (Au) and sacrificial silver (Ag) segments (Au–Ag–Au or Au–Ag–Au–Ag–Au) using the electrochemical wet etching method is reported. The nanorods were fabricated using an alumina template of thickness 100 μm and pore size of 200 nm. A variety of nanorods from single to seven segments comprising alternate Au and Ag segments were fabricated with better control of growth rate. The multisegment nanorods were selectively etched by removing the Ag segments to create gaps in the fabricated nanorods. A careful investigation led to the creation of a wide variety of nanogaps in the fabricated multisegment nanorods. The size of the nanogap was controlled by the passage of current through the electrochemical process, and size below 10 nm was achievable at exchanged charges of $\sim$1 mC. A further lowering in the size of nanogaps was achieved by diluting the silver plating solution and a segmented nanorod with nanogap (Au–nanogap–Au) of 3.8 nm at exchanged charges of 0.2 mC was successfully created. In addition, segmented nanorods with two or more nanogaps (Au–nanogap–Au–nanogap–Ag) placed symmetrically and asymmetrically on either side of the central Au segments were also created. A prototype of a single-electron transistor device based on segmented nanorods with two nanogaps is proposed. The results obtained could form the basis for the realization of quantum tunneling devices where the barrier thickness is very critical and demands values less than 5 nm. The encouraging results show the promise of multisegment nanorods for fabricating devices working at the de Broglie wavelength such as single-electron transistors.

(Some figures in this article are in colour only in the electronic version)

1. Introduction

The discovery of tunneling of a single electron and Coulomb blockade phenomena [1, 2] in the 1980s jolted the physics of field effect transistors, and such discoveries gave a new direction to developing future transistors obeying single-electron instructions. This attracted a wide range of attention and since then single-electron transistors (SETs) have been one of the most active areas of research. Though such devices perform only at low temperatures, however, their features are strong enough to revolutionize the present and future electronic sciences. SETs have shown to be potential candidates as elements for future low power, high density integrated circuits and memory devices [3–6] because of their potential for

[1] Author to whom any correspondence should be addressed.

ultra-low power operation involving only a few electrons. However, there are still considerable challenges before reaching these milestones. In order to be useful in practical applications, SETs must be functional at room temperature. Another challenge is to fabricate ultra-small tunneling junctions for high temperature operation, for which the fabrication process has been generally complicated and difficult to reproduce [7]. The SETs consist of a small conducting island connected to two electron reservoirs through tunnel barriers [6] which are conventionally referred to as tunneling nanogaps. Capacitance and thermal fluctuation limitations require that the island size of the SETs be no larger than ∼10 nm, a feature size outside the range of present conventional microfabrication processes [3–5]. There are several methods to fabricate nanosegments and nanogaps needed for the device geometry of SETs such as electromigration, shallow angle evaporation, electron-beam lithography and dip-pen lithography [8–11].

The synthesis of one-dimensional multisegment nanostructures has received steadily growing interest due to their peculiar and fascinating properties gaining a wide range of applications in biotechnology such as biosensing [12], gene delivery [13] and catalysts [14] as well as in optoelectronics aspects like photodetectors [15] and light-emitting diodes [16]. Several alternatives for multicomponent nanorod fabrication have been demonstrated, including the vapor phase method [17–21], template-direct synthesis [22, 23] and other methods [24–28]. However, fabrication of such multisegment nanorods are directed to high complexity in techniques and high cost in processing due to usage of enhanced deposition equipment such as pulsed-laser deposition (PLD), chemical vapor deposition (CVD) and metal–organic vapor phase epitaxy (MOVPE) [17]. The multisegment nanorods synthesized by template-direct fabrication, especially the electrochemical plating technique, is recognized as an outstanding effective approach due to its low cost fabrication, simplicity and high uniformity of the end product. Moreover, the nanorods can be flexibly tailored through a multiple choice of individual segment composition by using distinct plating solutions.

In the present work, electrochemical deposition is used to grow cylindrical multisegment nanorods of gold (Au) and silver (Ag) such as Au–Ag–Au or Au–Ag–Au–Ag–Au. The conditions are optimized to grow segmented nanorods with nanogaps and their growth characteristics and potential applications for single-electron transistors have been discussed.

2. Experimental details

2.1. Growth of single (Au/Ag) and multisegment (Au–Ag–Au) nanorods

Multisegment nanorods comprising Ag and Au segments were synthesized using electrochemical deposition using a porous anodized aluminum oxide (AAO) membrane (Whatman International Ltd, diameter = 25 mm, pore size = 200 nm). A thin layer of Ag (200 nm) was thermally evaporated on one side of the membrane to act as a cathode or working electrode in the chronoamperometry process carried out with Autolab PGSTAT30 equipment. Platinum wire and Ag/AgCl serve as counter and reference electrodes, respectively, in a three-electrode cell for the electrodeposition process. The Ag and Au nanorods were electroplated from the Technic ACR silver RTU solution (Technic Inc.) and Orotemp 24 RTU gold solution (Technic Inc.), respectively. A constant potential of −0.95 V was maintained between the working and the reference Ag/AgCl electrodes throughout the electrochemical process. For the uniformity of the cathode surface, a thin sacrificial Ag layer is grown on the interior of the AAO by exchanging 500 mC charges in the electrochemical process. When examined by scanning electron microscopy (SEM), the Ag layer thickness was ∼2 μm. This was followed by the electrochemical deposition of Au at exchanged charges of 250 mC, which led to deposition of ∼1 μm long Au nanorods. The thickness of the Au nanorods can be tuned by controlling the flow of exchanged charges through the electrochemical process. The electrochemical process is terminated here if only one-segment Au nanorods are required. For the growth of multisegment nanorods, Au and Ag layers are alternately grown and the thickness of these segments can be controlled by monitoring the flow of charges through the electrochemical process. The various steps involved in the fabrication of multisegment nanorods (Au–Ag–Au) are shown in figure 1(a). The middle Ag segment was grown at different exchanged charges from 0.5 to 50 mC, depending on the requirements. It was noticed that 3 mC of exchanged charges corresponded to 30 nm, 1 mC to 9–10 nm and 0.8 mC to 7–8 nm thickness of Ag segments. To make electrical contacts on the multisegment nanorods, we made sure that the end Au segments of the multisegment nanorods (Au–Ag–Au) were grown at 250 mC exchanged charges corresponding to a thickness of ∼1 μm. After the growth of multisegment nanorods the AAO template is treated with concentrated nitric acid for 5 min to remove the thermally deposited Ag and sacrificial Ag layer. Now the AAO template having multisegment gold nanorods in its interior is mixed with 3 M sodium hydroxide solution for 45 min. Sodium hydroxide dissolves the AAO template and the final product left is multisegment nanorods. The nanorods were then cleaned by continuous repeated centrifugation and rinsed with deionized water until the resultant solution reached a pH value of 7.

2.2. Creating nanogaps in multisegment nanorods

The method of creating nanogaps in the fabricated multisegment nanorods is illustrated in figure 1(b). For making the gap in the grown multisegment nanorods, the Au–Ag–Au nanorods were first dispersed in ethanol and subsequently transferred onto a passivated silicon wafer. The silicon wafer was heated at 90 °C for 1 min in air to vaporize the ethanol, followed by dropping saturated 11-mercaptoundecanoic acid (MUA) and heating at 200 °C for 20 min for incubation. Finally, concentrated nitric acid was added to the incubated multisegment nanorods (Au–Ag–Au) to etch out the middle Ag segment to leave behind the segmented Au nanorods with a nanogap. The saturated MUA solution is considered as

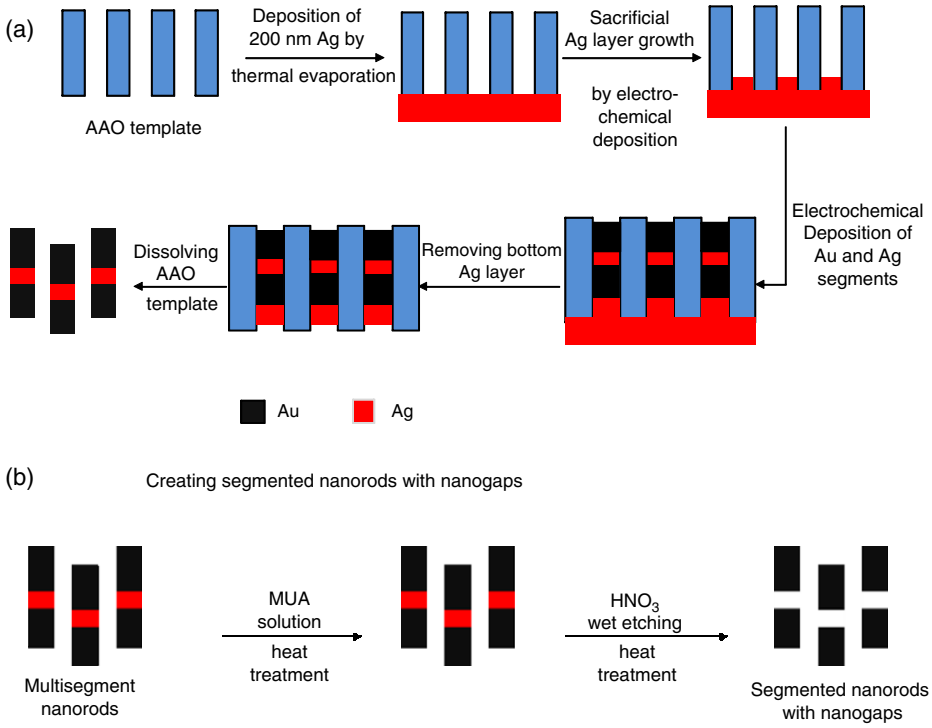

Figure 1. (a) Steps involved in the fabrication of multisegment nanorods; (b) creating nanogaps in the fabricated multisegment nanorods.

sticky material to hold the segments of nanorods intact even when the MUA-coated nanorods are chemically reacting with concentrated nitric acid [29]. The nanorod segments do not move during the selective etching because the heat treatment effectively removes the MUA coating and immobilizes the nanorods. This completes the process of making nanogaps in the multisegment nanorods.

2.3. Electrode fabrication

The Au electrodes used in the present work were designed using Autocad software. The designed mask consists of arrays of electrode units with each unit (2 mm × 2 mm) consisting of ten pairs of electrodes, and the thickness of each electrode and the separation between them is 2 μm. The designed mask consists of 475 units to be patterned on a passivated silicon wafer of 4 inch diameter. Optical lithography and lift-off techniques were used to fabricate the Au electrodes. The passivated silicon wafer was cleaned using acetone, isopropanol and DI water and, after heat treatment at 90 °C for 1 min, a positive photoresist (AZ 5214E) was spin-coated at a speed of 4000 rpm. The photoresist-coated wafer was then soft-baked at 110 °C for 1 min to remove solvent, stress and to promote adhesion of the resist layer on the wafer. The resist-coated wafer was UV-exposed for 25 s using Mask Aligner (Karl Suss MA6). The exposed wafer was incubated at 115 °C for 1 min, followed by post-exposure with UV for 135 s. The post exposed wafer is treated with developer (MIF 500) solution for 2–3 min, till the photoresist patterns are developed. Chromium (25 nm) and Au (200 nm) are subsequently deposited on the photoresist-patterned wafer by thermal evaporation. The Au electrodes were formed on the silicon wafer by lift-off removal of the photoresist. Finally, the fabricated chips having Au electrodes were diced and were ready for use in studying the I–V characteristics of multisegment nanorods. The grown multisegment nanorods (Au–Ag–Au) were dispersed on fabricated chips using a micropipette and the chips were heat treated at 90 °C for 1 min in air to vaporize the ethanol. To make sure that the nanorods make good contacts with the Au electrodes, MUA solution was added drop-wise onto the chips and heated at 200 °C for 20 min for incubation. The chips were examined under optical microscopy to scan the position of nanorods for performing I–V measurements. The chips carrying multisegment nanorods are treated with nitric acid to remove the middle Ag segment and were used to study and compare the I–V characteristics of segmented nanorods with a nanogap (Au–nanogap–Au) and multisegment nanorods (Au–Ag–Au).

I–V characteristics were carried out using a Keithley I–V measurement unit (Model-4200-FCS). The fabricated multisegment nanorods were examined by scanning electron microscopy (SEM) (JEOL, Model: JSM-7401F). X-ray diffraction (XRD) (Bruker AXS, Model: D8 FOCUS) was used to examine the crystallinity of grown nanorods. Energy-dispersive x-ray spectroscopy (EDS) was used to detect the trace levels of Ag/Au segments in the fabricated multisegment nanorods.

3. Results and discussion

3.1. Characteristics of multisegment nanorods

The grown multisegment nanorods were characterized for their crystallographic orientation using the x-ray diffraction (XRD)

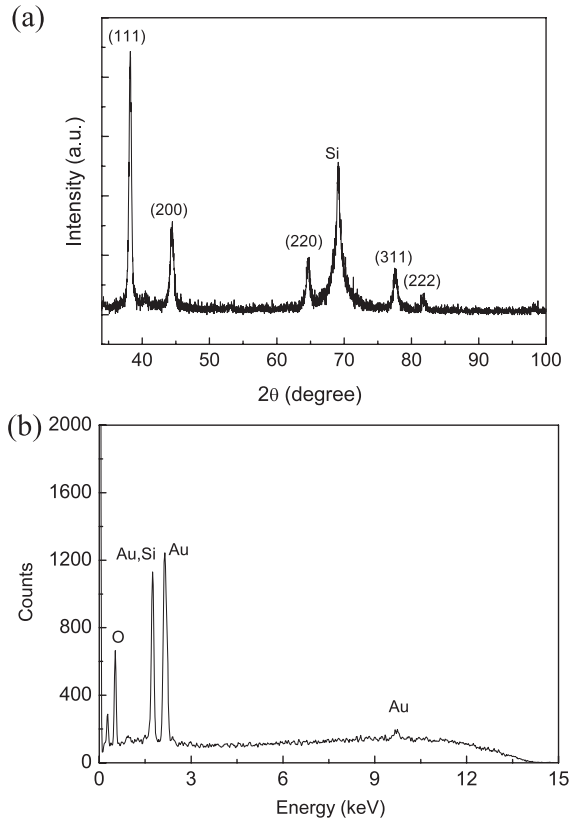

Figure 2. (a) XRD spectrum of Au nanorods; (b) EDS spectrum of Au nanorods (Si and O peaks are emanating from the oxidized silicon substrate).

technique as shown in figure 2. In the XRD profile, peaks corresponding to (111), (200), (220), (311) and (222) of metallic Au are resolved. These peaks are consistent with the Joint Committee on Powder Diffraction standards (JCPDS 04-0784) and other published works [30–32]. Furthermore, the preferred orientation along the (111) plane indicates that the grown nanorods can be readily indexed to face centered cubic Au. It may be noted that other Bragg reflections are comparatively weak and considerably broadened relative to the (111) reflection, which indicates that Au nanorods are anisotropic in shape. No peak characteristics of any impurities were observed, indicating the high quality growth of Au nanorods. This was further confirmed by investigating the chemical composition of the grown materials using EDS. The EDS spectrum shows the peaks corresponding to metallic Au only and thus confirms the growth of pure Au nanorods (figure 2(b)). Other peaks corresponding to O and Si emanate from the substrate (SiO_2/Si).

The road to the realization of a single-electron transistor using multisegment nanorods requires an optimization of the conditions for fabricating segmented Au nanorods with nanogaps. The size of the nanogap is very critical in the design of SETs and requires values less than 10 nm. Therefore, we optimized the condition for growing multisegment nanorods (Au–Ag–Au) with varying thickness of the middle Ag sacrificial layer. Figure 3 shows the SEM images of the fabricated segmented Au nanorods with different nanogaps. The middle Ag segment was grown at different exchanged charges of 4 mC, 3 mC, 1 mC and 0.7 mC, which after selective etching resulted in the formation of segmented Au

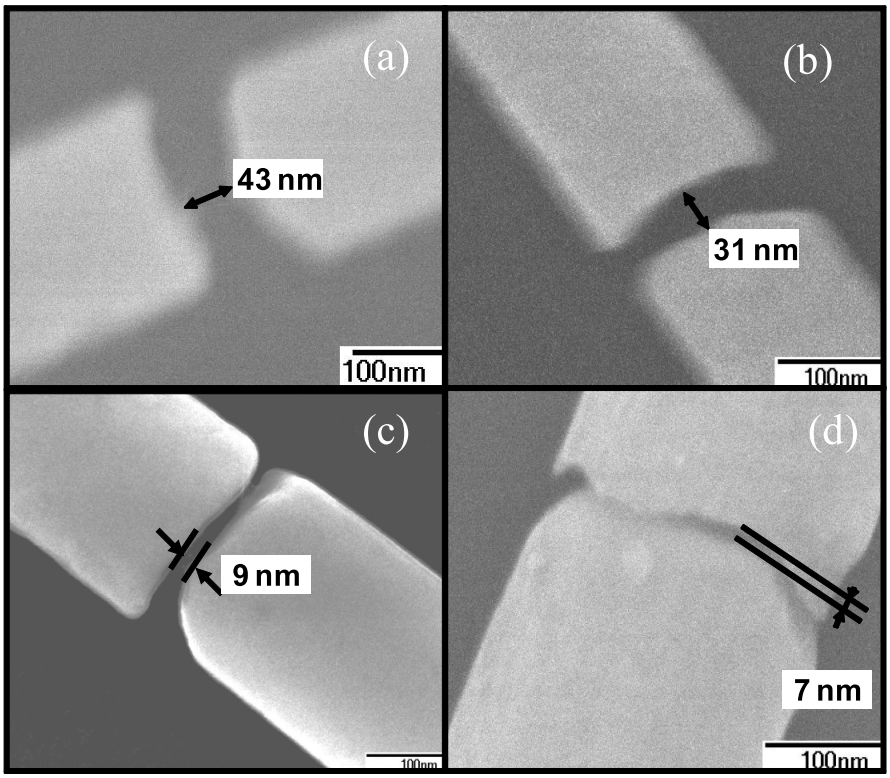

Figure 3. SEM images depicting the segmented nanorods with nanogap (d) corresponding to different exchanged charges (Q): (a) $d = 43$ nm for $Q = 4.0$ mC; (b) $d = 31$ nm for $Q = 3.0$ mC; (c) $d = 9$ nm for $Q = 1.2$ mC; and (d) $d = 7.0$ nm for $Q = 0.78$ mC.

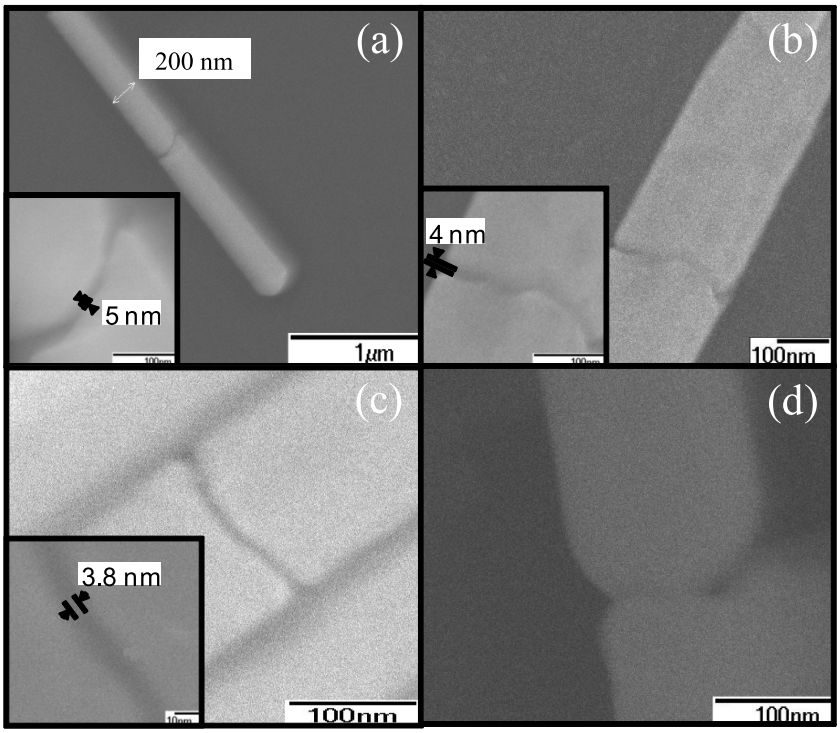

Figure 4. SEM images depicting the segmented nanorods with nanogap (d) corresponding to different exchanged charges (Q): (a) $d = 5.0$ nm for $Q = 0.5$ mC; (b) and (c) correspond to $d = 4.0$ nm for $Q = 0.4$ mC and $d = 3.8$ nm for $Q = 0.2$ mC, respectively; (d) the SEM image is not clear at $Q \sim 0.1$ mC due to the limitation of SEM resolution.

nanorods with nanogap sizes of 43 nm, 31 nm, 9 nm and 7 nm, respectively (figures 3(a)–(d)). It is important to mention that a nanogap below 10 nm is not only difficult to fabricate but also challenging to image by SEM. It may be noticed that SEM images are blurred and this may be due to the presence of MUA coating across the nanorods. Another factor which influenced and restricted the formation of nanogaps below 7 nm was the concentration of the Ag solution. At high concentration (as purchased from the company), the time required to pass 0.7 mC of exchanged charges through the electrochemical process was too short so that within a few seconds (1–2 s) the said amount of charges were consumed for the Ag segment growth. Therefore, it was necessary to increase the operating time and at the same time reduce the growth rate. Therefore, the Ag plating solution was diluted with DI water (1:10) and it was found that dilution of the Ag plating solution allowed the satisfactory electroplating of Ag at the minimum exchanged charges of ∼0.2 mC. Figure 4 shows the SEM images of segmented nanorods with nanogaps of 5 nm, 4.0 nm and 3.8 nm, corresponding to exchanged charges of 0.5 mC, 0.4 mC and 0.2 mC, respectively. The Ag plating was also performed at ∼0.1 mC exchanged charges, but we could not observe a clear image due to the resolution limit of the SEM (figure 4(d)). At such a small scale of less than 5 nm the presence of Ag cannot be completely ignored even after selective etching using concentrated nitric acid. Therefore, we performed the EDS of samples of segmented nanorods with nanogaps of 3.8 nm to find out the possibility of the presence of Ag. Figure 5 shows the EDS spectrum taken around the 3.8 nm gap (also refer to the inset, figure 5). The peaks corresponding

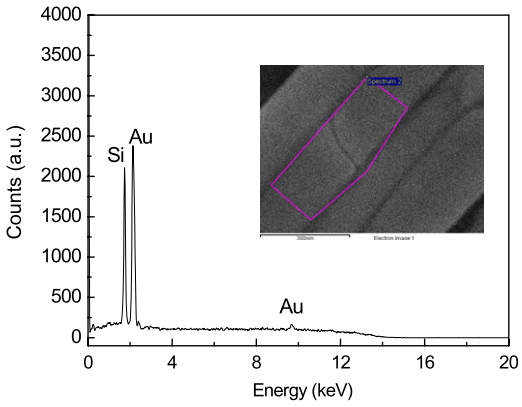

Figure 5. The EDS signals obtained on segmented Au nanorods with a nanogap of 3.8 nm. Inset shows the SEM image of the nanogap area selected for taking EDS spectrum.

to Au and Si (wafer) are clearly visible; however, the absence of an Ag peak confirms the formation of a gap between the Au segments and indicates the complete removal of Ag.

3.2. I–V measurements

In this section we present the room temperature I–V characteristics of a single Au nanorod, multisegment nanorod (Au–Ag–Au) and segmented nanorods with nanogap. For the I–V measurements nanorods suspended in ethanol were dispersed on passivated silicon chips prefabricated with Au electrodes using the method described in section 2.3.

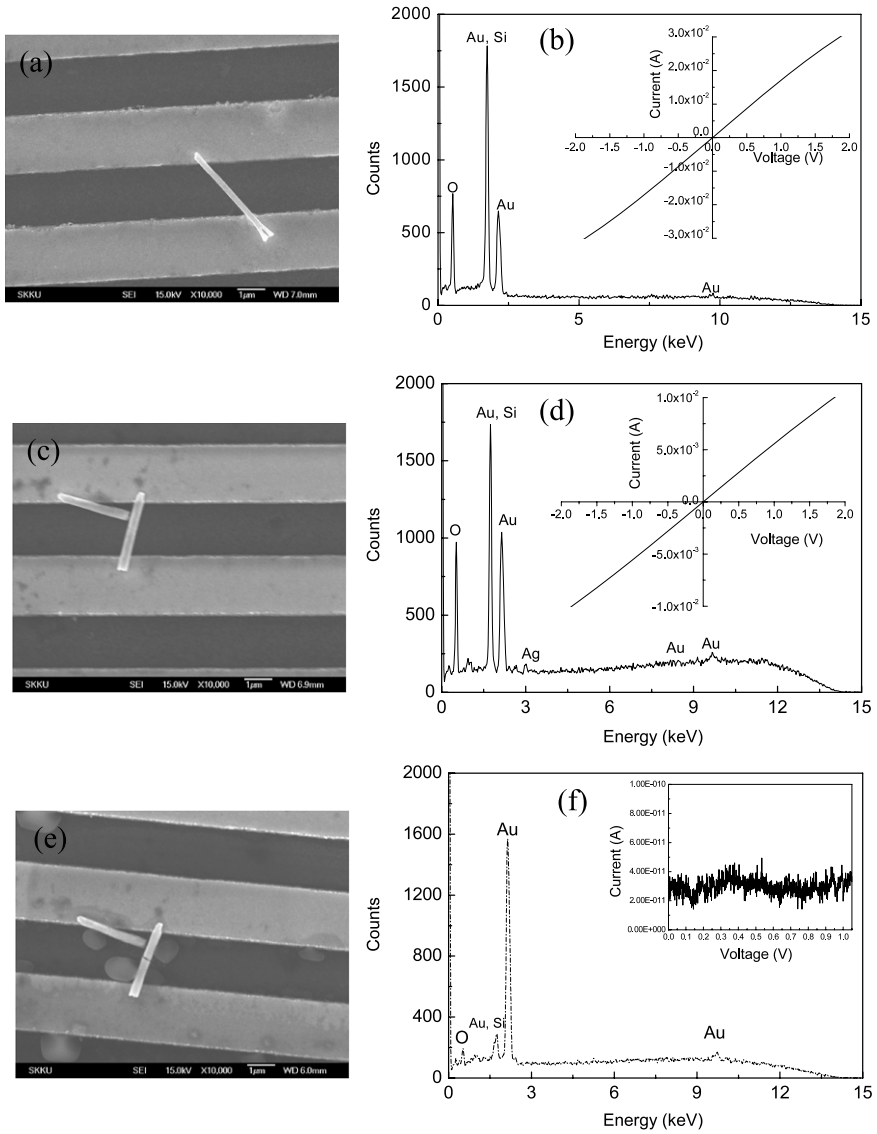

Figure 6. SEM images and characteristics of pure Au nanorod, multisegment nanorod and segmented Au nanorods with nanogap: (a) SEM image of Au nanorod between a pair of Au electrodes; (b) EDS spectrum of a single Au nanorod. Inset of (b) shows the I–V curve of a single Au nanorod exhibiting linear ohmic behavior; (c) SEM image of multisegment nanorod (Au–Ag–Au) between a pair of Au electrodes; (d) EDS spectrum of multisegment nanorod (Au–Ag–Au) showing the peaks corresponding to Au and Ag (Si and O peaks are emanating from the substrate (SiO_2/Si)). Inset of (d) shows the I–V characteristic of multisegment nanorod (Au–Ag–Au) exhibiting linear ohmic behavior; (e) SEM image of segmented nanorods with nanogap (Au–nanogap–Au) between a pair of Au electrodes; (f) I–V curve of segmented Au nanorods with nanogap. Inset of (f) shows the EDS spectrum of segmented Au nanorods with nanogap exhibiting peaks corresponding to Au segments only. This confirms the formation of a nanogap without traces of Ag.

Figure 6(a) shows the SEM image of a one-segment Au nanorod placed between two Au electrodes. Figure 6(b) depicts the EDS spectrum of an Au nanorod indicating the nanorod is composed of Au only. The peaks corresponding to Si and O are emanating from the substrate SiO_2/Si. The inset of figure 6(b) is showing the I–V characteristic of a one-segment Au nanorod exhibiting linear behavior and indicates that the Au nanorod formed good ohmic contacts with the Au electrodes. After this, multisegment nanorods (Au–Ag–Au) were examined for the continuity of grown materials along the length of the nanorods by measuring the I–V characteristic. Figure 6(c) shows the SEM image of a multisegment nanorod (Au–Ag–Au) placed between two Au electrodes, and the EDS spectrum indicates the presence of Au and Ag segments (figure 6(d)). The inset of figure 6(d) shows the linear I–V characteristic indicating: (a) the three segments form a continuous nanorod without any breaks at the interface of different segments; (b) contacts to the Au electrodes are ohmic and (c) grown multisegment nanorods are metallic and continuous.

After selectively etching the middle Ag segment from the multisegment nanorod (Au–Ag–Au), EDS and I–V measurements were performed. Figure 6(e) shows the SEM image of segmented Au nanorods with a nanogap (Au–nanogap–Au) placed between a pair of Au electrodes. The EDS spectrum of the segmented nanorods with a nanogap

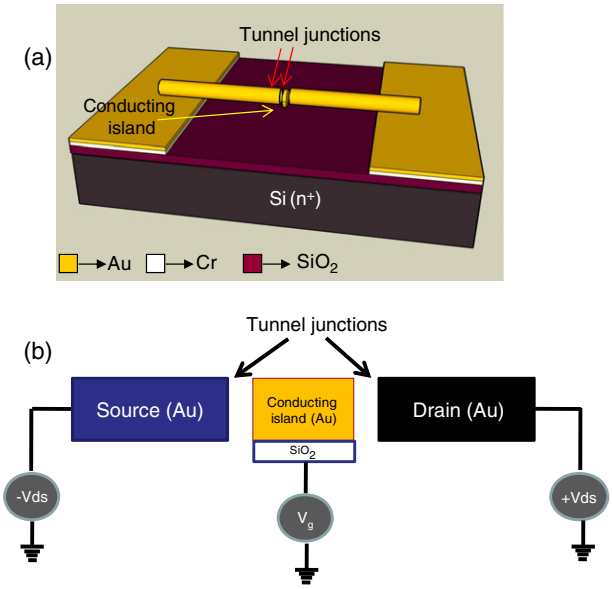

Figure 7. (a) Schematic diagram of the proposed SET structure based on segmented Au nanorods with two nanogaps (Au–nanogap–Au–nanogap–Au) assembled on passivated highly doped (n^+) silicon substrate. The end Au segments are placed on a pair of Au electrodes having a separation of 2 μm between them; (b) shows the prototype of the proposed SET design.

shows the peaks corresponding to Au segments only and thus confirms the formation of a nanogap and complete etching of the Ag segment (figure 6(f)). The I–V measurement was performed at room temperature and naturally current ceases to flow at such a wide gap (14 nm) and the expected behavior is shown in the inset of figure 6(f). This further indicates that Ag is completely removed from the nanogap. For the tunneling behavior to be observable the conditions that need to be met are barrier thickness less than 5 nm and cryogenic temperatures. The present study concludes that (a) Au nanorods form the ohmic contacts with Au electrodes by treating with MUA solution and (b) removal of Ag from the multisegment nanorods by selective etching is confirmed by both EDS and I–V measurement techniques.

3.3. Proposed SET structure and its growth

The segmented nanorods with a nanogap discussed so far have to be modified for their potential application in quantum tunneling devices like SETs. SETs consist of a small conducting island connected to two electron reservoirs through tunnel barriers [6] which are conventionally referred to as tunneling nanogaps. Moreover, the barrier thickness and width of the conducting island are the deciding factors for the design of SETs. The electron tunneling, needed for SET operation, is observable at cryogenic temperatures for barrier thicknesses less than 5 nm. Therefore, SETs not only demand careful engineering but very low operating temperatures. The present work proposes a device structure using a very economical, cost-effective and reliable approach of electrochemical plating which can be used to fabricate the elements of SETs. Figure 7 shows the prototype of an SET device using segmented nanorods with two nanogaps on a passivated highly doped silicon (n^+) substrate. The structure of SETs can be realized in terms of segmented Au nanorods with two nanogaps (Au–nanogap–Au–nanogap–Au) in the following manner: the central Au segment could serve as the conducting island, the two nanogaps on either side as tunnel barriers and the Au segments on the extremes as electron reservoirs (figure 7). Having said this, it is important to optimize the condition for the growth of segmented Au nanorods with two or more gaps. In the present work, three types of segmented nanorods (Au–nanogap–Au–nanogap–Au) with two nanogaps were fabricated; two segmented nanorods with symmetrically placed nanogaps and one with asymmetrically placed nanogaps. In the first case, two types of segmented nanorods with symmetric nanogaps were fabricated: one type was fabricated with both Ag segments grown at exchanged charges of 1.6 mC; and the other type of segmented nanorods was fabricated with both Ag segments electroplated at 0.5 mC exchanged charges. In the second case, the segmented nanorods with asymmetric nanogaps were fabricated by growing the Ag segments at exchanged charges of ~0.8 and 1.4 mC, respectively. The middle Au segment in the case of all fabricated multisegment nanorods (Au–Ag–Au–Ag–Au) was grown at fixed exchanged charges of 2 mC, which corresponds to a thickness of 20 nm. The end Au segments of the multisegment nanorods were grown at 250 mC exchanged charges, which corresponds to a thickness of 1 μm. Figures 8(a)–(c) show the SEM images of the fabricated segmented nanorods with two nanogaps: (a) segmented nanorods with two symmetric nanogaps of 16 nm each (Au–nanogap–Au–nanogap–Au = 1 μm–16 nm–20 nm–16 nm–1 μm); (b) segmented nanorods with two asymmetric nanogaps of 14 and 8 nm (Au–nanogap–Au–nanogap–Au = 1 μm–14 nm–20 nm–8 nm–1 μm); and (c) segmented nanorods with two symmetric nanogaps of 5 nm each (Au–nanogap–Au–nanogap–Au = 1 μm–5 nm–20 nm–5 nm–1 μm). The image in figure 8(c) is blurred due to the resolution limit of the SEM at such a low scale. The growth of segmented nanorods with three nanogaps or multisegment nanorods with seven segments was also attempted and the Ag segments were grown at 1.4 mC exchanged charges, the inner Au segments at 50 mC exchanged charges and the end Au segments were electroplated at 250 mC exchanged charges. Figure 8(d) shows the SEM image of segmented nanorods with three nanogaps of 14 nm each. Thus, we see that multisegment nanorods of different dimensions and nanogaps less than 5 nm can be fabricated by the electrochemical wet etching process. The present study reveals that multisegment nanorods have a great future in a wide variety of applications ranging from nanoelectronics to exposing the rich underlying physics in these grown segmented nanorods with nanogaps by (1) studying the transport properties at the dimension of the de Broglie wavelength and (2) studying the tunneling current and realizing devices based on tunneling phenomena. The electrochemical growth of multisegment nanorods seems advantageous and convenient than with available techniques which are either costly or require sophistication. The final product yield is very high and results are consistent, reproducible and reliable. The electrical behavior and

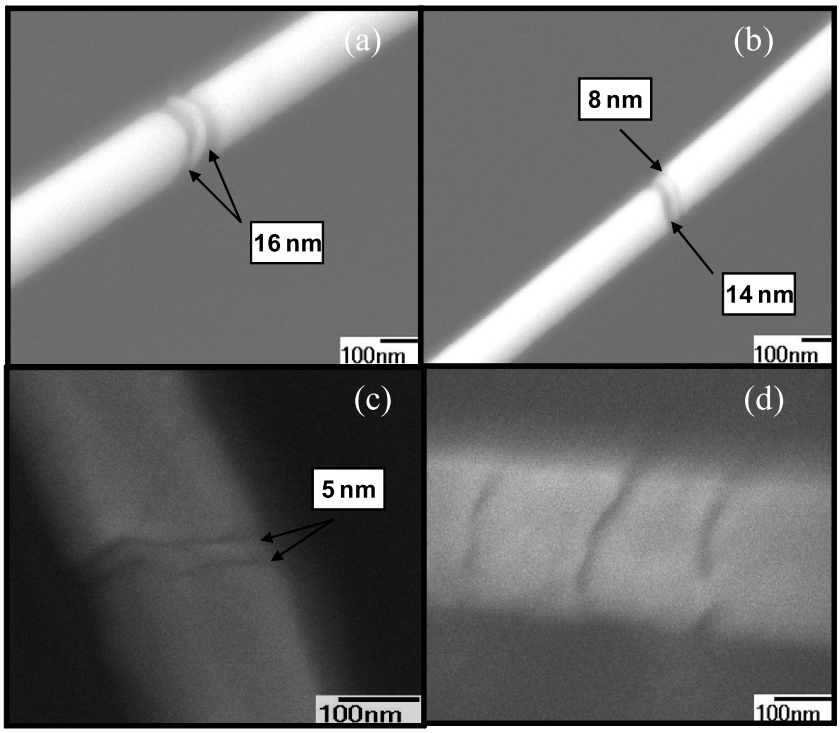

Figure 8. SEM images showing the segmented nanorods with two and three nanogaps. (a)–(c) show the SEM images of the fabricated segmented Au nanorods with two nanogaps: (a) segmented nanorods with two symmetric nanogaps of 16 nm each (Au–nanogap–Au–nanogap–Au = 1 μm–16 nm–20 nm–16 nm–1 μm); (b) segmented nanorods with two asymmetric nanogaps of 14 nm and 8 nm (Au–nanogap–Au–nanogap–Au = 1 μm–14 nm–20 nm–8 nm–1 μm); (c) segmented nanorods with two symmetric nanogaps of 5 nm each (Au–nanogap–Au–nanogap–Au = 1 μm–5 nm–20 nm–5 nm–1 μm); and (d) shows the SEM image of segmented Au nanorods with three nanogaps of 14 nm each.

device performance of the proposed SET device based on segmented nanorods (Au–nanogap–Au–nanogap–Au) is under active investigation and will be published elsewhere.

4. Conclusion

We have demonstrated the fabrication of segmented nanorods with nanogaps using the electrochemical wet etching technique. Segmented nanorods with a nanogap down to 3.8 nm have been fabricated. Such a low dimension of nanogaps could be fabricated by controlling the passage of exchanged charges through the electrochemical process. The results show the immense potential of one-dimensional segmented nanorods with nanogaps for various applications, such as a convenient means to study the I–V characteristics of biological particles such as DNA and ferritin and, more importantly, studying the I–V characteristics of segmented nanorods with nanogaps to investigate the tunneling effect at cryogenic temperatures for single-electron transistor applications.

Acknowledgments

The authors are grateful to Professor Sungho Park and Mr. Sang-Hoon Yo for useful discussions and technical help. This work was supported by the Korea Science and Engineering Foundation (KOSEF) Grant funded by the Korea Government (MOST) (R01-2006-000-10065-0).

References

[1] Fulton T A and Dolan G J 1987 *Phys. Rev. Lett.* **59** 109
[2] Klein D L and Roth R 1997 *Nature* **389** 699
[3] Devoret M H and Schoelkopt R J 2000 *Nature* **406** 1039
[4] Nakazato K, Blaikie R J, Cleaver J R A and Ahmed H 1993 *Electron. Lett.* **29** 384
[5] Tucker J R 1992 *J. Appl. Phys.* **72** 4399
[6] Likharev K K 1999 *Proc. IEEE* **87** 606
[7] Kang L, Chae D H and Yao Z 2007 *Nanotechnology* **18** 465203
[8] Park H, Alivisatos A P and McEuen P L 1999 *Appl. Phys. Lett.* **75** 30
[9] Lefebvre J, Radosavljevic M and Johnson A T 2000 *Appl. Phys. Lett.* **76** 3828
[10] Liu K, Avouris Ph, Bucchignano J, Martel R, Sun S and Michl J 2002 *Appl. Phys. Lett.* **80** 865
[11] Zhang H, Chung S W and Mirkin C A 2003 *Nano Lett.* **3** 43
[12] Penn S G, He L and Natan M L 2003 *Curr. Opin. Chem. Biol.* **7** 609
[13] Salem A K, Searson P C and Leong K W 2003 *Nat. Mater.* **2** 668
[14] Lee K B, Park S and Mirkin C A 2004 *Angew. Chem.* **116** 3110
[15] Mcalpine M C, Friedman R S and Lieber C M 2005 *Proc. IEEE* **93** 1357
[16] Hayden O, Agarwal R and Lieber C M 2006 *Nat. Mater.* **5** 352
[17] Mieszawska A J, Jalilian R, Sumanasekera G U and Zamborini F B 2007 *Small* **3** 722

[18] Xia Y, Yang P, Sun Y, Wu Y, Majors B, Gates B, Yin Y, Kim F and Yan H 2003 *Adv. Mater.* **15** 353
[19] Lauhon L J, Gudiksen M S and Lieber C M 2004 *Phil. Trans. R. Soc.* A **362** 1247
[20] Law M, Goldberger J and Yang P 2004 *Annu. Rev. Mater. Res.* **34** 84
[21] Samuelson L 2003 *Mater. Today* **6** 22
[22] Brumlik C J and Martin C R 1999 *J. Am. Chem. Soc.* **113** 3174
[23] Isaacs L, Chin D N, Bowden N, Xia Y and Whitesides G M 1999 *Supermolecule Technology* ed D N Reinhoudt (New York: Wiley) pp 1–46
[24] Hornyak G, Kröll M, Pugin R, Sawitowski T, Schmide G, Bovin J O, Karsson G, Hofmeister H and Hopfe S 1997 *Chem.—Eur. J.* **3** 1951
[25] Zhang Y, Ichihashi T, Landree E, Nihey F and Iijima S 1999 *Science* **285** 1719
[26] Park B, Ryu Y and Yong K 2004 *Surf. Rev. Lett.* **11** 373
[27] Ostermann R, Li D, Yin Y, McCann J T and Xia Y 2006 *Nano Lett.* **6** 1297
[28] Park S, Lim J-H, Chung S-W and Mirkin C A 2004 *Science* **303** 348
[29] Shuhong L, Jeffrey B H T and Zhenan B 2005 *Nano Lett.* **5** 6
[30] Kuo C H, Chiang T F, Chen L J and Huang M H 2004 *Langmuir* **20** 7820
[31] Huang C-J, Chiu P-H, Wang Y-H, Yang C-F and Feng S-W 2007 *J. Colloid Interface Sci.* **306** 56
[32] Liu F-K, Huang P-W, Chang Y-C, Ko C-J, Ko F-H and Chu T-C 2005 *J. Cryst. Growth* **273** 439